Available online at www.sciencedirect.com
ScienceDirect
Applied Thermal Engineering 27 (2007) 779–787
APPLIED THERMAL ENGINEERING
www.elsevier.com/locate/apthermeng

Transonic turbine blade loading calculations using different turbulence models – effects of reflecting and non-reflecting boundary conditions

S. Djouimaa [a,*], L. Messaoudi [b], Paul W. Giel [c]

[a] Physical Department, Sciences Faculty, Batna University, Ave Chahid Boukhlouf Med, El-Hadi, 05000 Batna, Algeria
[b] Mechanical Department, Engineering Sciences Faculty, Batna University, Ave Chahid Boukhlouf Med, El-Hadi, 05000 Batna, Algeria
[c] QSS Group, Inc., NASAGlenn Research Center Cleveland, OH 44135, USA

Abstract

The objective of this study is to simulate the transonic gas turbine blade-to-blade compressible fluid flow. We are interested mainly in the determination of the pressure distribution around the blade. The particular blade architecture makes these simulations more complex due to the variety of phenomena induced by this flow.

Our study is based on the experiment performed by Giel and colleagues. Tests were conducted in a linear cascade at the NASA Glenn Research Center. The test article was a turbine rotor with design flow turning of 136° and an axial chord of 12.7 cm.

Simulations were performed on an irregular quadratic structured grid with the FLUENT software package which solves the Navier–Stokes equations by using finite volume methods. Two-dimensional stationary numerical simulations were made under turbulent conditions allowing us to compare the characteristic flow effects of Reflecting Boundary Conditions (RBC) and Non-Reflecting Boundary Conditions (NRBC) newly implemented in FLUENT 6.0. Many simulations were made to compare different turbulence models: a one equation model (Spalart–Allmaras), several two-equation models (k–ε, RNG k–ε, Realizable k–ε, SST k–ω), and a Reynolds-stress model (RSM). Also examined were the effects of the inlet turbulence intensities (0.25% and 7%), the exit Mach numbers (1.0 and 1.3) and the inlet Reynolds numbers (0.5×10^6 and 1×10^6). The results obtained show a good correlation with the experiment.

Keywords: Transonic gas turbine; Turbulent conditions; RBC and NRBC Effects

1. Introduction

For several decades, the gas turbines have been the subject of several works linked especially to the comprehension and internal flow characterisation and identification in order to make these machines more adapted for the environment and more optimal. Transonic turbines constitute particularly a very interesting study case because of the complexity needed to model the internal flow which passes, through the blades, from subsonic to supersonic conditions with an eventual shock appearance.

Many researchers [1–4,15] are particularly interested in the experimental study in order to provide precise data for CFD codes validations which are currently largely used by industry.

With efficiency and power increases of modern gas turbines, researchers tried continuously to increase the inlet temperature to the maximum. This can be done only with better blade cooling, great heat transfer comprehension and three-dimensional distribution of the temperature inside the turbine. To give a detailed cooling analysis as well as a good thermal structure of blades, several researchers treated numerically the three-dimensional flow which has very important effects, in particular the secondary flows, for the heat transfer in a real turbine [5–7,12,15,19].

* Corresponding author. Tel.: +213 33 85 45 15; fax: +213 33 86 14 06.
E-mail address: sihemdjouimaa@univ-batna.dz (S. Djouimaa).

1359-4311/$ - see front matter © 2006 Elsevier Ltd. All rights reserved.
doi:10.1016/j.applthermaleng.2006.10.018

Nomenclature

C_x	blade axial chord [m]	Pt	total pressure [P_a]
Re_{C_x}	Reynolds number based on C_x		
M_{is}	isentropic mach number	*Subscripts*	
Tu	turbulence intensity	in	inlet freestream value
P	static pressure [P_a]	ex	outlet freestream value

Many authors [6,7,10,11,16–18] invested their efforts in the modelling and the two-dimensional flow comprehension. Indeed, seen the blade complex form, the flow is characterized by regions with large continuous pressure gradients causing strong accelerations and decelerations. Maciejewski and Moffat [13] and Thole and Bogard [14] showed that strongly turbulent flow coming from combustor causes an early boundary layer transition and increased heat transfer. Although Larsson et al. [11] developed methods for external heat transfer prediction in supersonic turbines, the major part of this article deals with details subsonic and transonic flow between blades.

As for modelling the flow, very good results were obtained, especially for transition [11], by the Baldwin–Lomax algebraic model for entrance turbulence intensities $Tu < 0.2\%$. But to model the influence of the higher values of Tu, only two equations models were used (Low–Re k–ε and k–ω). On the suction side, only the Launder–Sharma model is able to capture laminar region. All other models predict an almost immediate transition and a fully turbulent boundary layer on the whole suction side. All models used predicted too high turbulence levels around the leading edge. This excessive production of turbulence is caused by the large normal strains in the stagnation region [11]. On the pressure side, all models give quite good results. Concerning the trailing edge, all models give oscillations at the separation point, thing which is very difficult to avoid [7], this was confirmed by Giel et al. [1]. Many researchers have previously used boundary layer and Navier–Stokes solvers with algebraic turbulence models with good results, but these methods break down and are not good at predicting what happens at the leading edge, and they often have difficulties at the trailing edge due to separation. Furthermore, there are big problems with separated regions, shocks and high inlet turbulence levels. With a transport models, this problems can be solved or, at least, reduced. On the other hand, some authors have successfully used the commercial code FLUENT to simulate the flow in turbomachineries.

Before starting the thermal study, this work has as a principal objective to contribute to master internal flows by determining the pressure distribution around a rotor blade. Different turbulence models (Spalart–Allmaras, k–ε, RNG k–ε, Realizable k–ε, SST, k–ω, and RSM) are used in order to find the most appropriate model to predict the flow around such a complex geometry in particular in the trailing and leading edges. Soon, the details of transitional zone on the blade suction side will be presented in future paper.

All simulations done in this work are for stationary and two-dimensional flows. There were realized on an irregular quadratic structured grid (generated by the preprocessor GAMBIT) with the FLUENT software package which solves the Navier–Stokes equations by using finite volume methods. Turbulence models were used with inlet intensities (0.25% and 7%), exit Mach numbers (1.0 and 1.3) and the inlet Reynolds numbers (0.5×10^6 and 1×10^6). Also, we show the effects of Reflecting Boundary Conditions (RBC) and Non-Reflecting Boundary Conditions (NRBC), newly implemented in FLUENT 6.0, on the flow characteristics. The objective in formulating non-reflecting boundary conditions was to prevent spurious, non-physical reflections at inflow and outflow boundaries, so that the calculated flow field is independent of the location of the far-field boundaries. This leads to a greater accuracy and greater computational efficiency, since the computational domain can be more compact [20]. All our calculations were made on the midspan. The results validation is based on the experimental data provided by Giel: Research Center "Lewis Transonic Turbine Blade–NASA" Giel et al. [1].

2. Experimental data

The initial description of the facility was given by Verhoff et al. [8]. Subsequently, the cascade inlet section was analyzed and redesigned by Giel et al. [9]. Blade and cas-

Table 1
Blade and Cascade characteristics [1]

Geometric parameter	Value	Flow parameter	Value
Axial chord	12.7 cm (5.000 in)	Inlet Re_{C_x}	$0.977 \pm 0.028 \times 10^6$
Pitch	13.00 cm (5.119 in)	Exit Re_{C_x}	$1.843 \pm 0.060 \times 10^6$
Span	15.24 cm (6.000 in)	Inlet M_{IS}	0.383 ± 0.0006
True chord	18.42 cm (7.250 in)	Exit M_{IS}	1.321 ± 0.003
Stagger angle	41.54°	Inlet flow angle	63.6°
Throat diameter	3.358 cm (1.393 in)	Design flow turning	136°
Throat area: 1 passage	53.94 cm^2 (8.360 in^2)		
Leading edge diameter	2.657 cm (1.046 in)		
Trailing edge diameter	0.518 cm (0.204 in)		

cade details Giel et al. [1,5] are given in Table 1 with repeatabilities based on 95% confidence limits.

3. Governing equations

The CFD-code FLUENT offers different approaches for treating flows in turbomachines [24]. The equations used by the finite volume solver to model the flow are the compressible, Reynolds-averaged continuity, momentum and energy equations discretized in algebraic form.

4. Numerical methods

The study domain consists of one passage with an inlet zone located at 12.7 cm from the leading edge, it is limited by intrados (pressure side) in the upper and extrados (suction side) in the lower. The blade profiles were obtained by creating real edges from a given 143 points defining the blade geometry [1,5]. GAMBIT forms the edges in the shape of general NURBS curve of degree n which is a piecewise rational polynomial function, wherein the numerator and the denominator are non-periodic B-Splines of degree n. By default, GAMBIT employs a value of $n = 3$ (Fig. 1). (NURBS is a specific notation to Gambit it is describes how to create real curve from existing points) [24]. The irregular quadratic structured grid is generated by the pre-processor GAMBIT. According to this complex geometry, the grid is obtained using the PAVE scheme, the total nodes number is 24900 (Fig. 2), not all of the near-wall grid lines are shown in the figure for clarity. This grid, which gave us a high satisfaction (speed convergence and results qualities), was obtained after several attempting improvements concerning upstream and downstream zones.

We made use of "Coupled solution method" [24]. Using this approach, the governing equations are solved simultaneously i.e. coupled together. Governing equations for additional scalars will be solved sequentially. A control-volume-based technique is used that consists of:

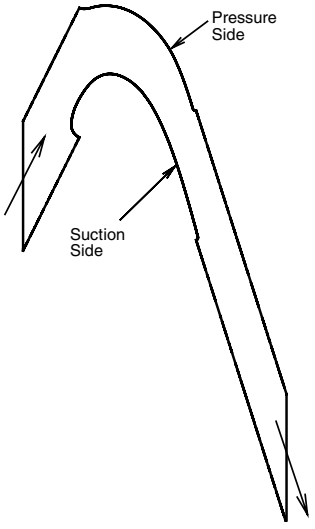

Fig. 1. Study domain.

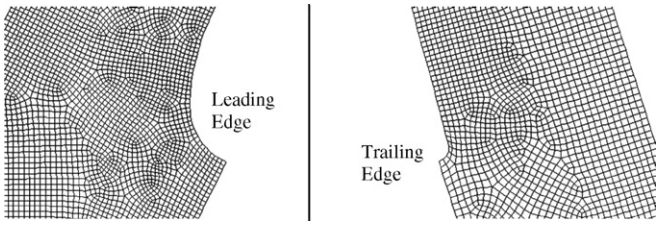

Fig. 2. Computational grid.

- Division of the domain into discrete control volumes using a computational grid.
- Integration of the governing equations on the individual control volumes to construct algebraic equations for the discrete dependent variables (unknowns) such as velocities, pressure, temperature, and conserved scalars.
- Linearization of the discretized equations and solution of the resultant linear equation system to yield updated values of the dependent variables.

The coupled approach is designed for high speed compressible flows and gives very satisfactory results in turbomachines especially with the implicit coupled solver. The second order upstream [24] scheme is used because a higher-order accuracy is desired.

5. Boundary conditions

The boundary conditions are very important to obtain an exact solution with a rapid convergence. According to the theory of characteristics, flow angle, total pressure, total temperature, and isentropic relations are used at the subsonic inlet. The same relations are used to determine the fluid properties at the supersonic outlet such as static pressure, static temperature and the isentropic exit Mach number.

- All the walls (pressure and suction sides) are considered adiabatic with no slip condition.
- Since the periodic boundaries are satisfied, instead of modelling the whole blades row of 11 passages of Giel et al. [1,5], only one passage is used in order to limit the computational time and costs.
- Total pressure, total temperature and the inlet flow angle are specified as the input conditions.
- Outlet static pressure is specified. Indeed, in FLUENT, one option in the numerical simulation is to set the static pressure at the outlet boundary as an invariant given by the input condition; the other option is to apply non-reflection treatment on the outlet boundary as it has been successfully applied on the far-field condition of the flow computation. Both of these methods are used in the present paper. Yao et al. [23] supported this by numerical results.

Pressure far-field conditions are used in FLUENT to model a free-stream condition at infinity, with free-stream Mach number and static conditions being specified (pressure and temperature). The pressure far-field boundary condition which is a NRBC is often called a characteristic boundary condition, since it uses characteristic information (Riemann invariants) to determine the flow variables at the boundaries [24].

6. Numerical simulations

Many simulations were made to show the characteristic flow effects of RBC and NRBCs compared with the experimental results of Giel et al. [1,5]. Also, a comparison is done with different turbulence models existing in FLUENT with near wall treatment accuracy required in order to determine which model must be able to account for all of the key physics correctly. FLUENT provides a one equation turbulence model (Spalart–Allmaras), several two-equation models (Standard k–ε, Renormalization-Group RNG k–ε, Realizable k–ε, Standard k–ω, SST k–ω), and a Reynolds-stress model RSM.

For the transonic flow, we have seen that it is necessary to simulate the inlet turbulence intensities (0.25% and 7%), the exit Mach numbers (1.0 and 1.3) and the inlet Reynolds effects (0.5×10^6 and 1×10^6) in the goal to prove the *FLUENT* software efficiency and approve the simulated results while comparing them with the experimental data.

All our simulations are done on a PC Pentium IV (2.8 GHz and 2 GB of RAM). The averaged convergence time by simulation which depends on the turbulence model is approximately 1 h 30 mn.

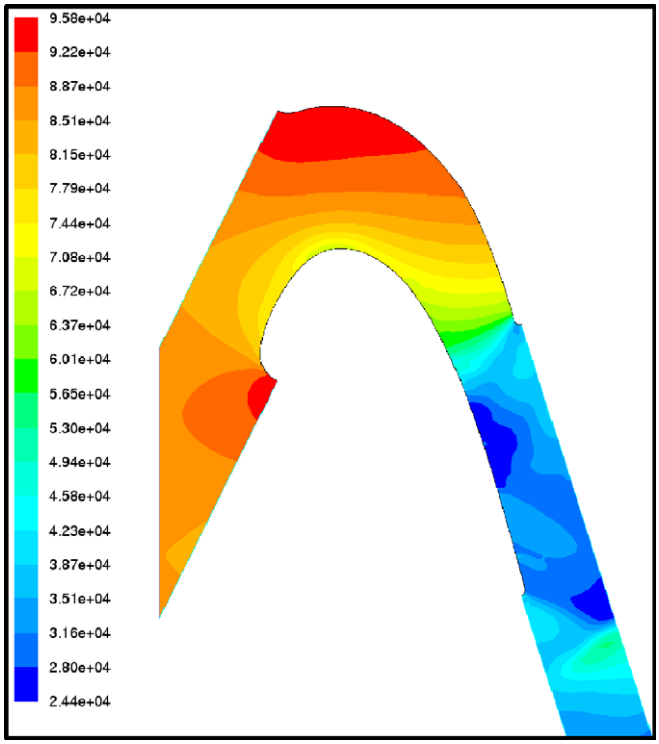

Fig. 3. Static pressure contours RBC.

7. Results

All calculations made in this paper are for the midspan. Results presented in Figs. 3–6 were obtained with RNG k–ε turbulent model ($Re_{in} = 1 \times 10^6$, $Tu = 0.25\%$ and $M_{ex} = 1.3$).

As mentioned below the objective in formulating non-reflecting boundary conditions was to prevent spurious, non-physical reflections at boundaries [20]. First, the simulation is done for an irregular quadratic structured grid of

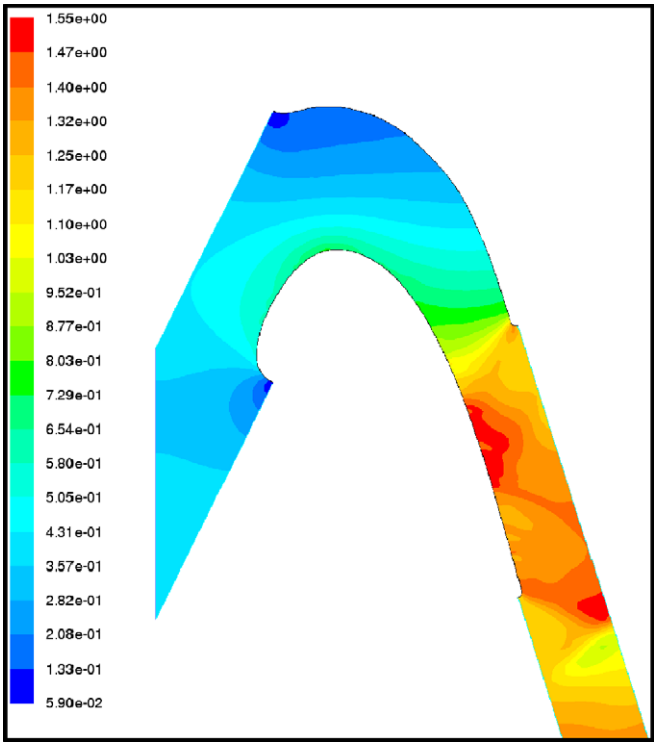

Fig. 4. Mach numbers contours RBC.

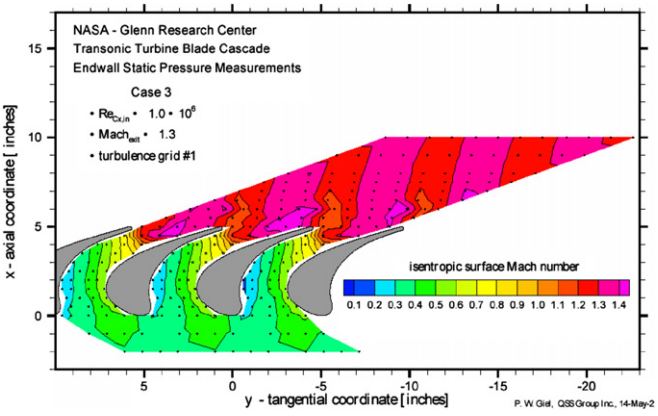

Fig. 5. Expérimental isentropic mach contours [P.W. Giel, Qss Group Inc,14 May 2001].

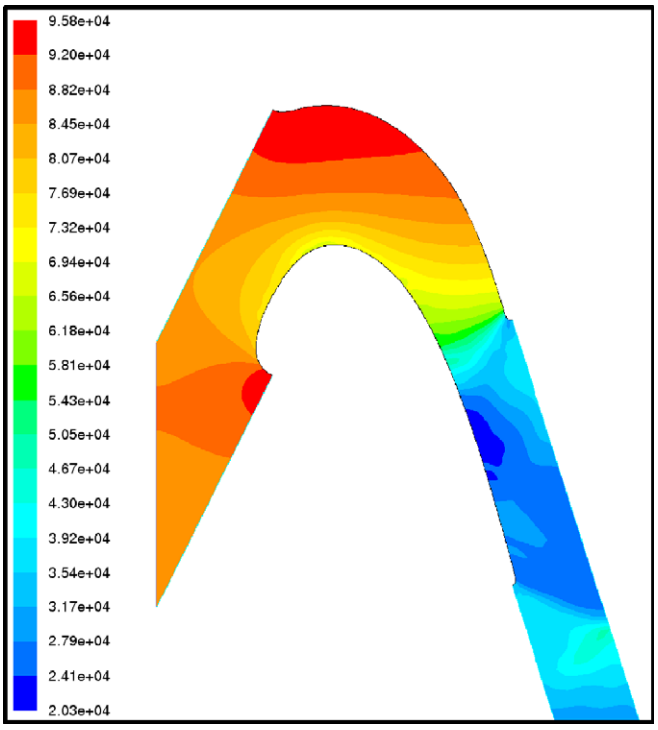

Fig. 6. Static pressure contours NRBC.

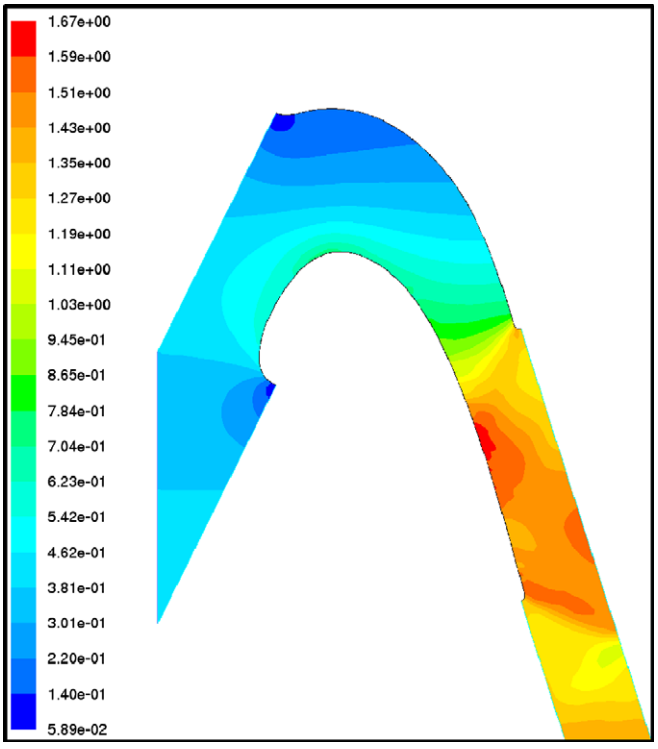

Fig. 7. Mach numbers contours NRBC.

7500 nodes. The objective was to find a solution for the shock reflection which is indicated by the darker blue stripe that starts just downstream of the lower blade trailing edge and emanates upward and to the right (Fig. 3).

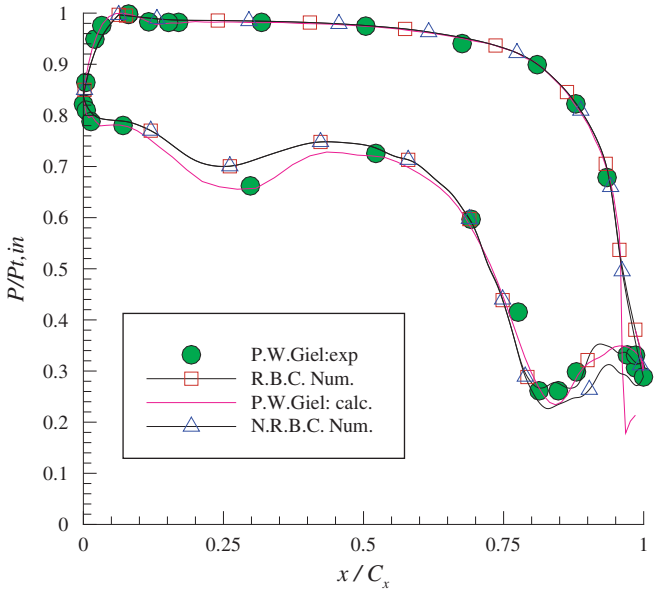

Fig. 8. Blade loading distribution RBC and NRBC comparison (7500 nodes).

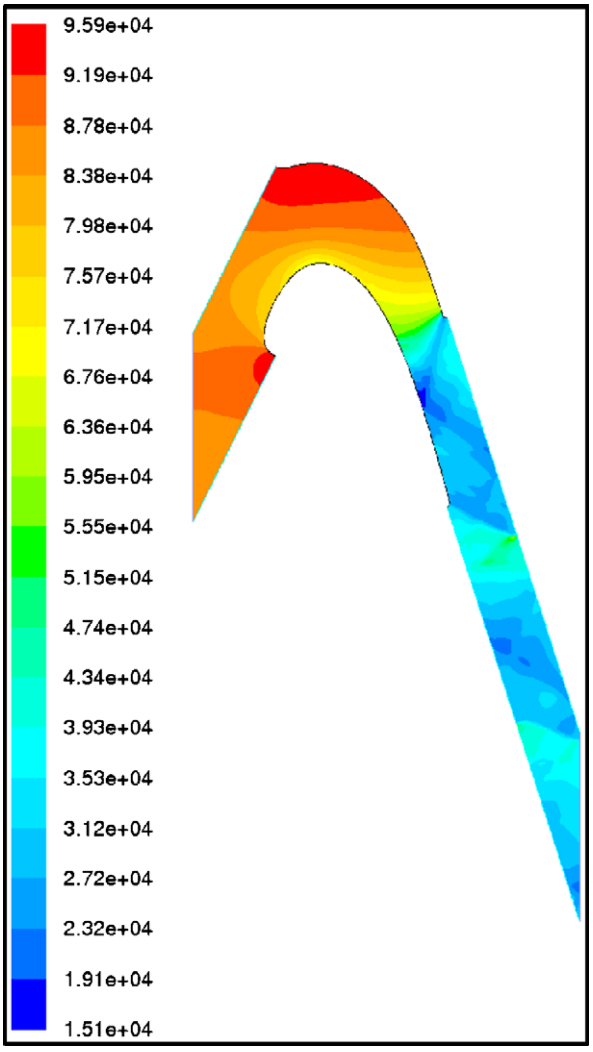

Fig. 9. Static pressure contours NRBC.

In comparing results with experiment (Fig. 5), we can see that the reflection is nonexistent, so the emanating stripe is spurious, which is also shown in (Fig. 4).

With a non-reflecting treatment applied to the outlet boundary (pressure far-field) the results are better when compared to experiments (Figs. 5 and 7). In (Fig. 8) in which we can see the RBC and NRBC comparison of blade loading distribution we can remark that the RBC results are a better match when comparing them with the experiment, but the NRBC results are closest to the previous 3-D numerical ones ($x/C_x = 0.8 \sim 1$). An erroneous pressure oscillation is seen in the RBC results near the minimum pressure location at $x/C_x \sim 0.85$.

Different self-adaptive sensors are applied in the grid refinement procedure for efficiently detecting the positions of the shock wave and the wake [21]. According to this, the shock wave is much sharper after the grid refinement; this is clearly seen in Figs. 9–12 which are obtained after refinement of the grid (24,000 nodes). This is also proved in comparing the Figs. 8 and 13.

Fig. 14 shows the blade loading distribution with a comparison of different turbulence models. We can see the excellent prediction of pressure distribution on the pressure side for all models which coincides perfectly with experimental values.

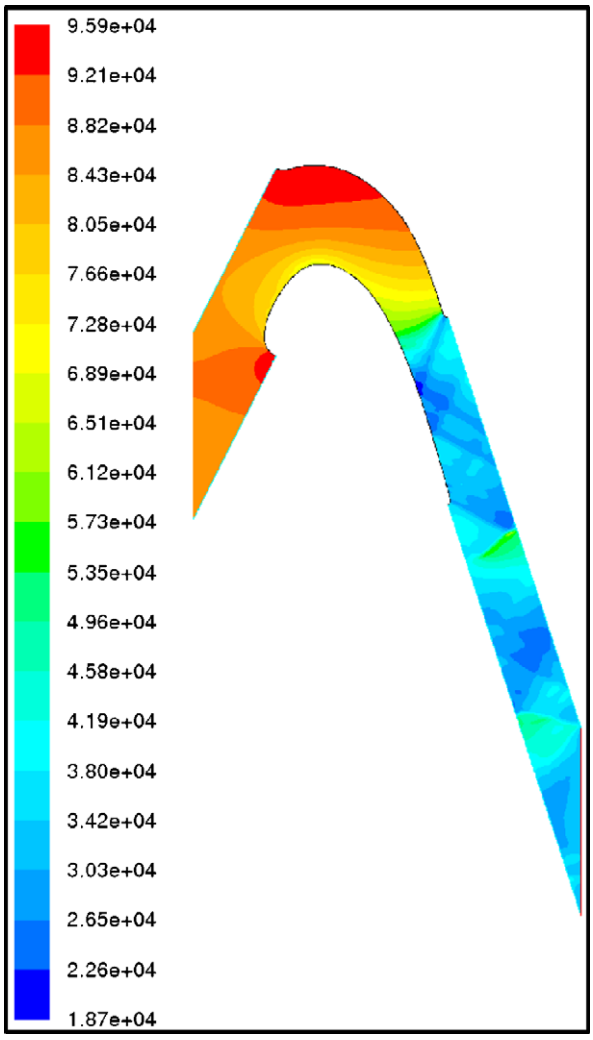

Fig. 10. Static pressure contours RBC.

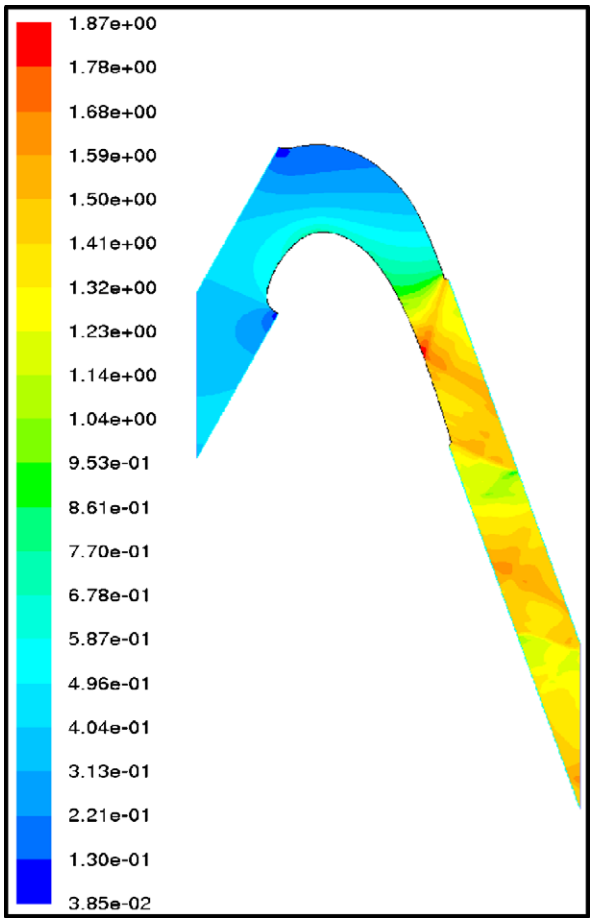

Fig. 11. Isentropic mach numbers contours NRBC.

On the suction side, some differences appears especially in the zone ($x/C_x = 0.05$–0.45) where the pressure gradients are important. Two equation eddy diffusivity models (EDMs) such as k–ε, k–ω and SST are the most widely used and the main reasons for this popularity are simplicity and robustness and although they do not account for some physics, they still provide useful insights [22].

Due to NASA blade shape [1], there is little margin for mistakes as we can see for the same zone k–ε and SST models predicts less the flow. The additional terms to the length-scale equation (ε or ω) make RNG and Realizable k–ε models account in a much better way for the influence of extra strain rates. The one equation model Spalart–Allmaras, designed especially for aerospace applications (boundary layers with adverse pressure gradients and turbomachinery), also gives good results the same as the RSM. model which has high potential for accurately predicting complex flows. The same comparisons can be made for the zone ($x/C_x = 0.8 - 1$) at the trailing edge and this is confirmed by the isentropic Mach number distribution (Fig. 15).

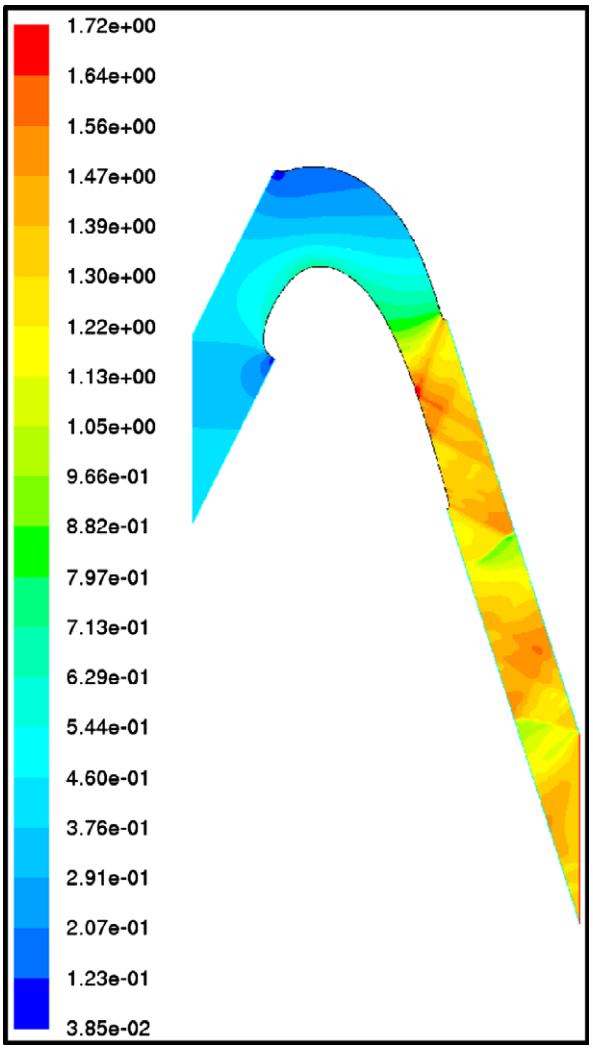

Fig. 12. Isentropic mach numbers contours RBC.

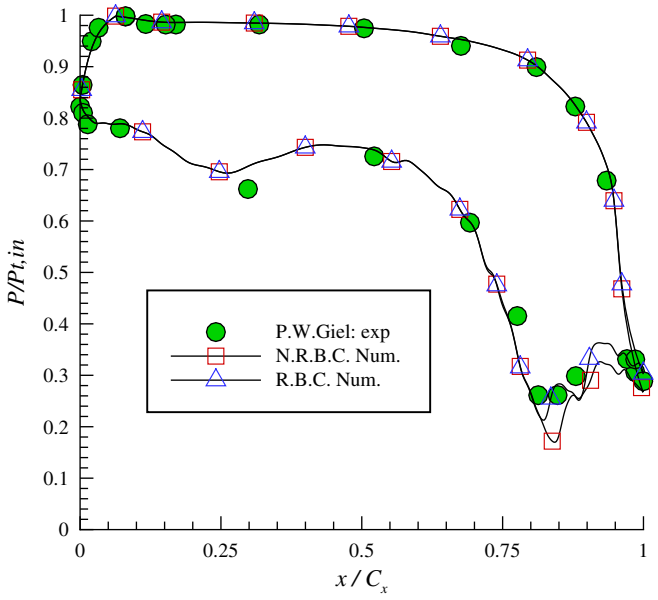

Fig. 13. Blade loading distribution. RBC and NRBC comparison (24,900 nodes).

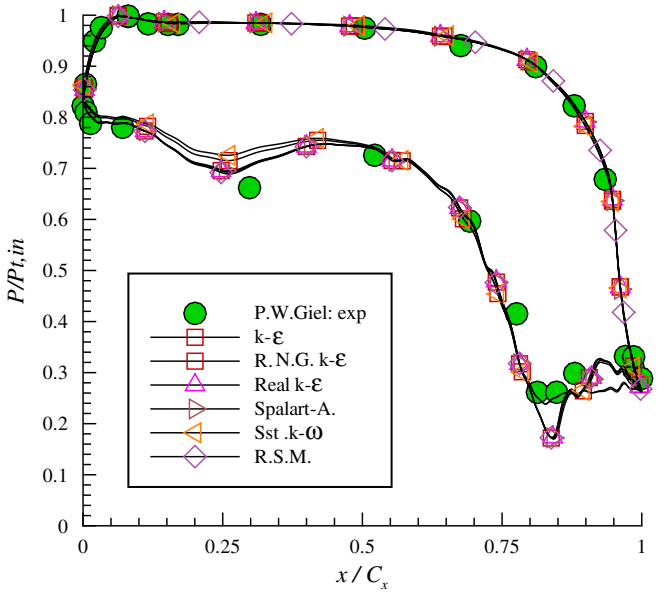

Fig. 14. Blade loading distribution. NRBC with different turbulence models comparison.

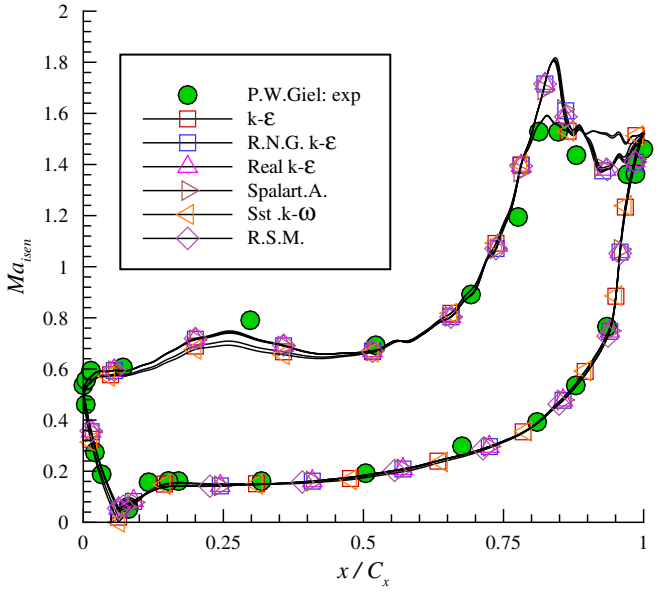

Fig. 15. Isentropic mach number distribution. NRBC with different turbulence models comparison.

The differences seen in experimental results with varying Tu (0.25% and 0.7%) (Fig. 16) are the same ones with computational results which prove the good precision of our simulations. Fig. 17 shows the Mach number contour ($Re_{in} = 1 \times 10^6$, $Tu = 0.25\%$ and $M_{ex} = 1.0$). In order to see the effects of decreasing exit Mach number, we can also see (Fig. 18) that it affects only the portion downstream the blade ($x/C_x = 0.7 - 1.0$). This is observed experimentally by Giel et al. [1].

To be noticed from Fig. 19 is that the Reynolds number has almost no effect on the pressure distribution and this was also confirmed by Giel et al. [1].

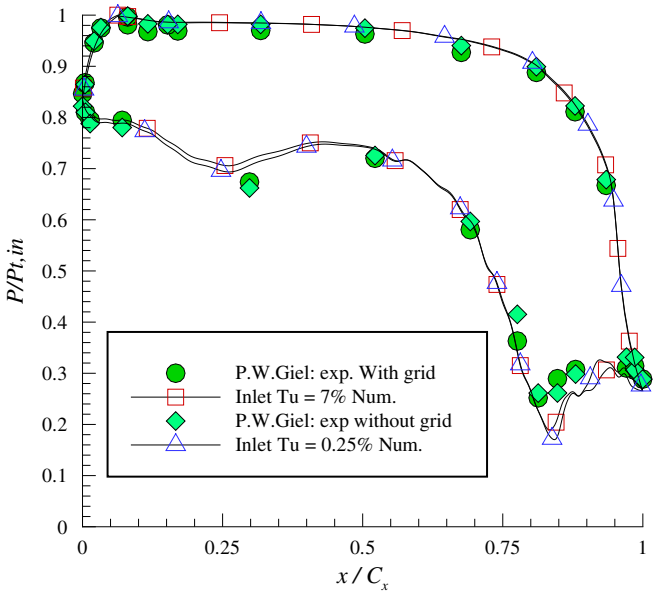

Fig. 16. Blade loading distribution. Inlet turbulence intensities effects.

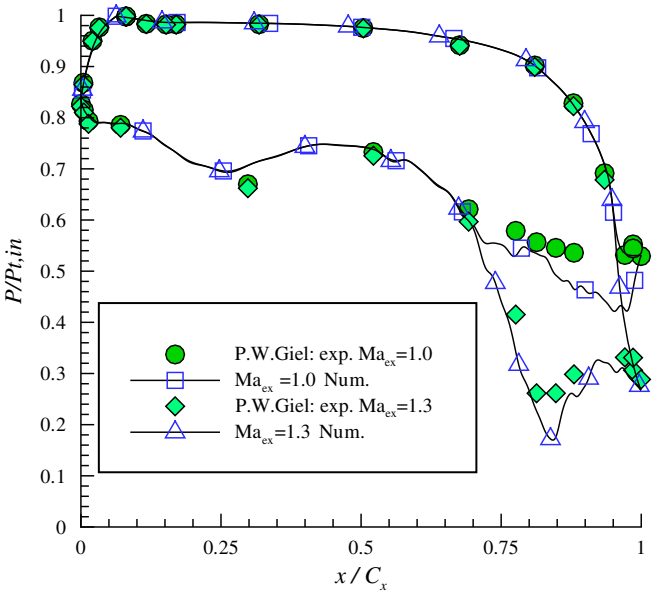

Fig. 18. Blade loading distribution. Ma_{ex} effects.

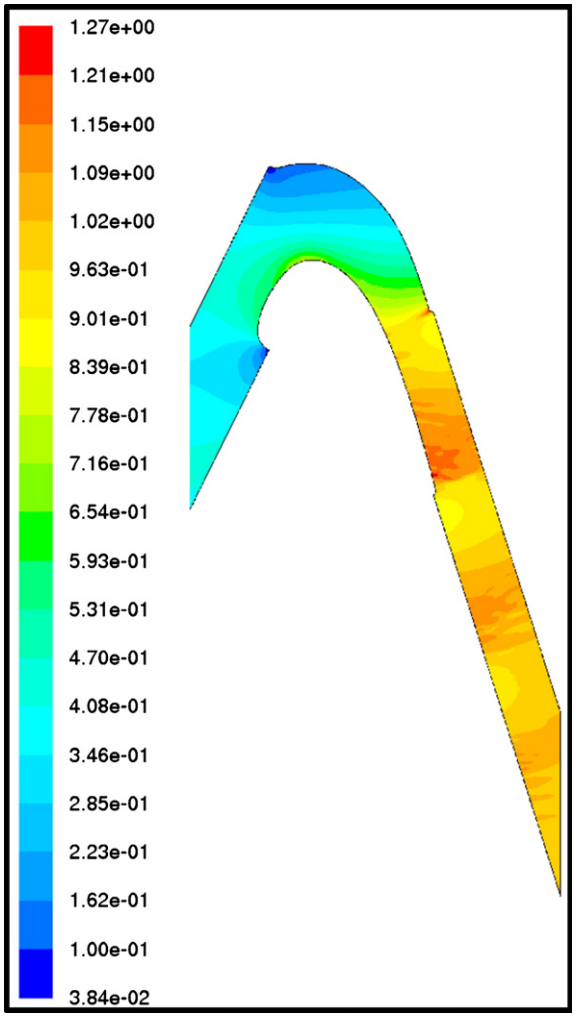

Fig. 17. Mach number contours Ma_{ex} effects.

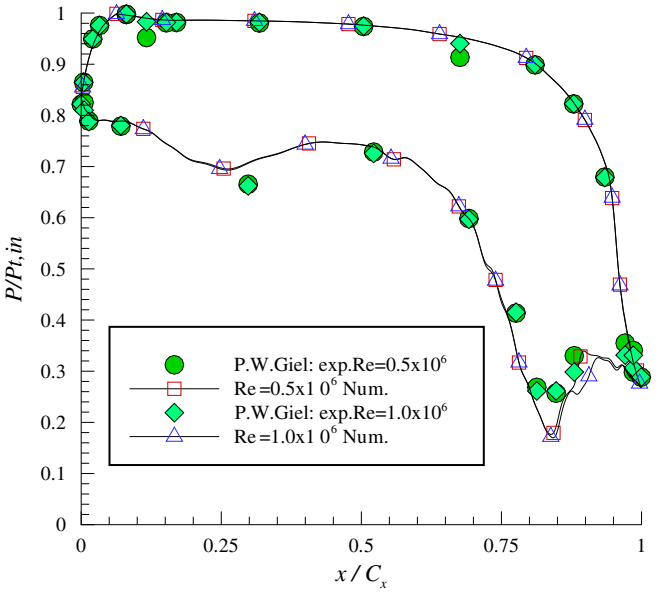

Fig. 19. Blade loading distribution. Inlet Reynolds effects.

8. Conclusion

Numerical simulations were made to determine the flow characteristics and mainly the pressure distribution around a transonic turbine blade. Much effort was invested in the grid in order to provide quality results. Several turbulence models were compared in order to determine which is the most appropriate model to predict this complex flow. Since our simulations show that the modified k–ε, the Spalart–Allmaras and the RSM models gives good results compared with experiment, instead to use all these models to determine the effects of reflecting and non-reflecting boundary conditions only the RNG model is selected, also

this model with NRBCs formulation is used to see the effects of the inlet turbulence intensities the exit Mach numbers and the Inlet Reynolds numbers. The results are closest to experiment. All the validations of results were made with those measured by Giel et al. [1].

Finally, we showed the capacity of ''FLUENT'' software package to predict the complex flow in a transonic turbine blade cascade. In spite of a long time to learn it, this software is equipped with very powerful pre-processing and post-processing modules.

Acknowledgements

First, we sincerely thank Dr. Paul W. Giel and Dr. Raymond Gaugler, Chief of the Turbine Branch – Turbomachinery and Propulsion Systems Division – NASA, for providing us their numerical and experimental results as well as the blade geometry. Without these data, we could not have achieved such results. Also, we thank Dr. P.W. Giel for providing us his articles and especially for guiding us throughout our work. We are very grateful to Dr. A. Ameri a researcher at NASA which was our first contact.

References

[1] P.W. Giel, D.R. Thurman, I. Lopez, R.J. Boyle, G.J. VanFossen, T.A. Jett, W.P. Camperchioli, H. La, Three-dimensional flow field measurements in a transonic turbine blade cascade, in: Proceeding of the ASME paper 96-GT-113, presented at the ASME International Gas Turbine Conference, June 10–13, Birmingham, England, 1996.

[2] R. Kiock, F. Lehthaus, N.C. Baines, C.H. Sieverding, The transonic flow through a plane turbine cascade as measured in four european wind tunnels, ASME Journal of Engineering Gas Turbine and Power 108 (1986) 277–284.

[3] D.J. Mee, N.C. Baines, M.L.G. Oldfield, T.E. Dickens, An examination of the contributions to loss on a transonic turbine blade in cascade, ASME Journal of Turbomachinery 114 (1) (1992) 155–162.

[4] C.G. Graham, F.H. Kost, Shock Boundary Layer Interaction on High Turning Transonic Turbine Cascades, ASME paper 79-GT-37, 1979.

[5] P.W. Giel, G.J. VanFossen, R.J. Boyle, D.R. Thurman, K.C. Civinskas, Blade heat transfer measurements and predictions in a transonic turbine cascade, ASME paper 99-GT-125, in: Proceeding of presented at the ASME International Gas Turbine Conference, Indianapolis, IN, June 7–10, 1999.

[6] Yumin Xiao, R.S. Amano, Analysis of flow and heat transfer in the end-wall region of a turbine blade passage, in; Proceeding of ASME TURBOEXPO 2000, 2000-GT-211, Munich, Germany, May 7–11, 2000.

[7] J. Larsson, Turbine blade heat transfer calculations using two-equation models, Department of Thermo and Fluid Dynamics, Chalmers University of Technology S-412 96 Gothenburg, Sweden, 1996.

[8] V.G. Verhoff, W.P. Camperchioli, I. Lopez, Transonic Turbine Blade Cascade Testing Facility, AIAA Paper No. 92-4034, NASA TM-105646, 1992.

[9] P.W. Giel, J.R. Sirbaugh, I. Lopez, G.J. VanFossen, Three-dimensional Navier–Stokes analysis and redesign of an imbedded bellmouth nozzle in a turbine cascade inlet section, ASME Journal of Turbomachinery 118 (1996) 529–535, July.

[10] C. Xu, R.S. Amano, Aerodynamics and heat transfer in a turbine blade at design and off-design angles of incidence, in: Proceeding of ASME TURBOEXPO 2000, 2000-GT-210, Munich, Germany, May 7–11, 2000.

[11] J. Larsson, L-E. Eriksson ,Ufl Hall, External heat transfer predictions in a supersonic turbines using the Reynolds averaged Navier–Stokes equations, in: Proceeding of the 12th ISABE Conference, Melbourne, vol. 2 (Copies distributed by AIAA), September 1995, pp. 1102–1112.

[12] M.F. Blair, An experimental study of heat transfer in a large-scale turbine rotor passage, ASME Journal of Turbomachinery 116 (1) (1994) 1–13.

[13] P.K. Maciejewski, R.J. Moffat, Heat transfer with very high free-stream turbulence: part i and ii, ASME Journal of Heat Transfer 114 (1992) 227–239.

[14] K.A. Thole, D.J. Bogard, Enhanced heat transfer due to high free-stream turbulence, ASME Journal of Turbomachinery 117 (1995) 418–424.

[15] Vijay K. Garg, Heat Transfer in Gas Turbines'', NASA/CR-2001-210942 AYT Research Corporation, Brook Park, Ohio, June 2001.

[16] Vogt, D.M., T.H. Fransson, A new turbine cascade for aerodynamical testing, in: Proceeding of the 16th Symposium on Measurement Techniques in Transonic and Supersonic Flow in Cascades and Turbomachines, Cambridge, UK, Sep. 2002.

[17] J Bredberg, Turbulence modeling for internal cooling of gas-turbine blades, Ph.D Thesis, Department of Thermo and Fluid Dynamics, Chalmers University of Technology, Göteborg, Sweden, 2002.

[18] Lars Davidson, An efficient and stable solution procedure of compressible turbulent flow on general unstructured meshes using transport turbulence models, AIAA 95-0342, in: Proceeding of the 33 rd Aerospace Sciences Meeting and Exhibit, January 9–12, Reno, NV, 1995.

[19] Björn Laumert, Hans Märtensson, Torsten H. Fransson, Investigation of the Flow-field in the transonic VKI Brite EURAM turbine stage with 3D steady and ansteady NS computations, in: Proceeding of the ASME TURBOEXPO 2000, Munich, Germany, May 8–11, 2000.

[20] Michael B. Giles, Non-reflecting boundary conditions for euler equation calculations, AIAA Journal 28 (12) (1990) 2050–2058.

[21] Y. Mei, A. Guha, Implicit numerical simulation of transonic flow through turbine cascades on unstructured grids, in: Proceeding of the IMechE., vol. 219, Part A: Journal of Power and Energy, A09404 © IMechE 2005, pp. 35–47.

[22] Tom I-P. Shih, Modeling and simulation of gas-turbine flow and heat transfer, Department of Mechanical Engineering, Michigan State University, East Lansing, MI 48824-1226, USA.

[23] J. Yao, A. Jameson, J.J. Alonso, F. Liu, Development and validation of massively parallel flow solver for turbomachinery flows, AIAA Paper, 00-00-0882, 2000.

[24] Fluent 6 User's Guide, 2001, Fluent Inc.